

## Inhomogeneous Superconductivity Induced in a Ferromagnet by Proximity Effect

T. Kontos, M. Aprili, J. Lesueur, and X. Grison

CSNSM-CNRS, Bât. 108, Université Paris-Sud, 91405 Orsay Cedex, France

(Received 7 September 2000)

Planar tunneling spectroscopy reveals damped oscillations of the superconducting order parameter induced into a ferromagnetic thin film by the proximity effect. The oscillations are due to the finite momentum transfer provided for Cooper pairs by the splitting of the spin-up and spin-down bands in the ferromagnet. As a consequence, for negative values of the superconducting order parameter the tunneling spectra are capsized (“ $\pi$  state”). The oscillations’ damping and period are set by the same length scale, which depends on the spin polarization.

DOI: 10.1103/PhysRevLett.86.304

PACS numbers: 74.50.+r

The quantum character of superconductivity arises from the existence of phase coherence in the electron condensate. In conventional superconductors, where pairing is provided by the exchange of virtual phonons, the phase is a constant. On the other hand, phase sensitive experiments [1] in high temperature superconductors have shown that the wave function of Cooper pairs with perpendicular quasiparticle momenta displays a  $\pi$ -phase shift suggesting unconventional pairing. Here, we show that a  $\pi$ -phase shift can also occur in the order parameter of conventional superconductors when superconducting correlations coexist with ferromagnetic order.

More than 30 years ago, Fulde and Ferrel [2] and Larkin and Ovchinnikov [3] (FFLO) showed independently that the superconducting order parameter may be modulated in real space by an exchange field. A Cooper pair, in the singlet state, acquires a finite momentum  $Q = 2E_{\text{ex}}/\hbar v_F$ , where  $2E_{\text{ex}}$  is the exchange energy corresponding to the difference in energy between the spin-up and spin-down bands, and  $v_F$  is the Fermi velocity. The superconducting phase grows linearly with the spatial coordinate  $x$ ,  $\varphi = Qx$  and a  $\pi$ -phase shift is expected for translations of  $\Delta x \approx \hbar v_F/4E_{\text{ex}}$ . Unlike high temperature superconductors, where  $\varphi$  is a  $2\pi$  multiple of 0 and  $\pi$ , in the FFLO state  $\varphi$  varies continuously.

The FFLO state occupies only a tiny part of the superconducting phase diagram close to the normal state [2]. The fragility of singlet superconductivity, when a finite exchange field removes the degeneracy of the ground state with respect to the spin degrees of freedom, makes the FFLO state difficult to ascertain experimentally. In bulk superconductors the normal state is recovered when  $E_{\text{ex}} > \sqrt{2}/2\Delta_s$  (Clogston criterion) [4], where  $\Delta_s$  is the superconducting energy gap. The situation is more favorable if Cooper pairs are injected from a superconductor into a ferromagnet  $F$  by the proximity effect. Assuming that the exchange field weakly affects the superconductor, superconducting correlations persist in  $F$  even for exchange energies much higher than  $\Delta_s$ . The physical reason is that Cooper pairs are not instantaneously broken when they penetrate the ferromagnet. They survive for a time corresponding to a traveled length on the order of  $\xi_F =$

$\hbar v_F/2E_{\text{ex}} = 1/Q$ , the coherence length scale in  $F$  [5], which is independent of the energy gap. The breakdown of the Clogston criterion turns out to be very significant since  $E_{\text{ex}}$  is typically at least 2 orders of magnitude larger than  $\Delta_s$ .

When a Cooper pair moves from a superconductor into a ferromagnet, the phase shift produces oscillations of the real part of the superconducting order parameter,  $\Psi$ , on a length scale given by  $\xi_F$  [5], as shown in Fig. 1(a) [6]. However, this artificially generated FFLO state vanishes on the same length scale, which is typically of the order of a few nm. Unlike bulk superconductors where the gap equation allows the FFLO state to occur only for exchange fields close to the critical field, this state exists for any exchange energy. We shall call the states corresponding to a positive sign of the real part of the order parameter the “0 state” and those corresponding to a negative sign of the order parameter the “ $\pi$  state.”

An induced superconducting order parameter in  $F$  modifies the quasiparticle density of states (DOS). In the  $\pi$  state, i.e., when the thickness of the ferromagnet is larger than  $\xi_F$ , the features in the superconducting DOS are reversed with respect to the normal state [6] [see inset of Fig. 1(a)]. This can be explained by considering the microscopic mechanism that allows superconducting correlations to propagate into  $F$ , i.e., Andreev reflections [7]. The process is illustrated in Fig. 1(b) using the energy-momentum dispersion law of the normal metal: An incoming electron in a normal metal  $N$  with energy lower than  $\Delta_s$  from the Fermi level is reflected into a hole at the  $S/N$  interface. The incoming electron and the outgoing hole accumulate a phase difference ( $\varphi = \Delta p \cdot x$ ) depending on their traveled distance,  $x$ , and on the difference between their momenta,  $\Delta p$ . Note that  $\Delta p$  is a function of the quasiparticle energy. If the normal layer is very thin, the phase difference is small and, roughly speaking, the DOS in  $N$  is close to that of the Cooper pair reservoir. The situation is strongly modified if the normal metal is ferromagnetic. As Andreev reflections invert spin-up into spin-down quasiparticles and vice versa [8,9], the total momentum difference includes the spin splitting of the conduction band:  $\Delta p_F = \Delta p + Q$  [see

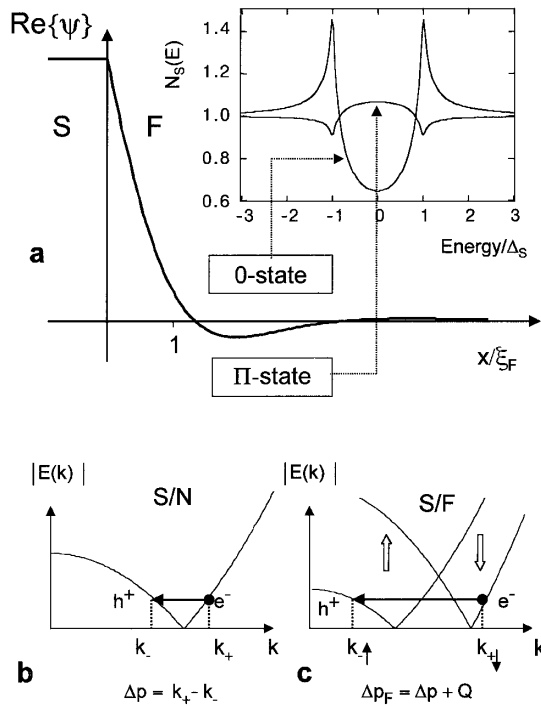


FIG. 1. (a) Exponentially damped oscillations of the real part of the superconducting order parameter induced into a ferromagnetic material by proximity effect. The space coordinate  $x$  denotes the distance from the superconductor/ferromagnet interface. The period of the oscillations is set by the coherence length  $\xi_F$ . 0 state and  $\pi$  state correspond to positive and negative signs of the real part of the order parameter, respectively. For the sake of simplicity, the superconductor is assumed unaffected by the exchange field of the ferromagnet  $F$ . Inset: superconducting density of states at zero temperature in the “0 and  $\pi$ ” states for an exchange energy  $E_{ex}$  much larger than the energy gap,  $\Delta_s$  [6]. The characteristic reversed shape in the  $\pi$  state is a consequence of the order parameter oscillations. (b) Schematic of the Andreev reflection process: an electron in the normal metal with momentum,  $k_+$ , is elastically reflected as a hole,  $k_-$ , at the superconductor/normal metal interface ( $S/N$ ). (c) If  $N$  is spin polarized, the momentum shift,  $\Delta p_F$ , is dominated by the spin splitting of the up and down bands.

Fig. 1(c)]. If the exchange energy is much larger than the energy gap, which is usually the case,  $\Delta p_F \approx Q$  and the phase difference between the electron and hole wave functions is almost energy independent. The DOS is modified in a thin layer on the order of  $\xi_F$ . In particular, the interference between the electron and hole wave functions produces an oscillating term in the superconducting DOS with period  $x E_{ex} / \hbar v_F$ . The oscillations turn the energy-dependent DOS upside down with respect to the normal state. Note that a phase-induced oscillating term in the superconducting DOS is a natural consequence of the coherent superposition of the electron and hole wave functions in a normal metal and has been observed as a function of energy in either the clean [10] or the dirty [11] limit.

We measure the superconducting DOS in a thin ferromagnetic film by tunneling spectroscopy. The normalized conductance vs bias of a normal-metal/insulator/

ferromagnet/superconductor ( $N/I//F/S$ ) junction probes the superconducting DOS induced in  $F$  by the proximity effect, convoluted by the thermal broadening [12]. The normalized conductance is defined as the bias-dependent conductance divided by the background conductance measured when both electrodes are in the normal state.  $Al/Al_2O_3/Pd_{1-x}Ni_x/Nb$  junctions were fabricated entirely *in situ* by thin film evaporation, with shadow masks defining the junction geometry [see inset of Fig. 2(a)]. The normal metal ( $N$ ) is Al in its normal state. The Nb and  $Pd_{1-x}Ni_x$  (hereafter called PdNi) are the Cooper pair reservoir ( $S$ ) and the ferromagnetic thin film ( $F$ ), respectively. Samples were  $e$ -gun evaporated in a typical base pressure of  $10^{-9}$  torr, with film thicknesses being

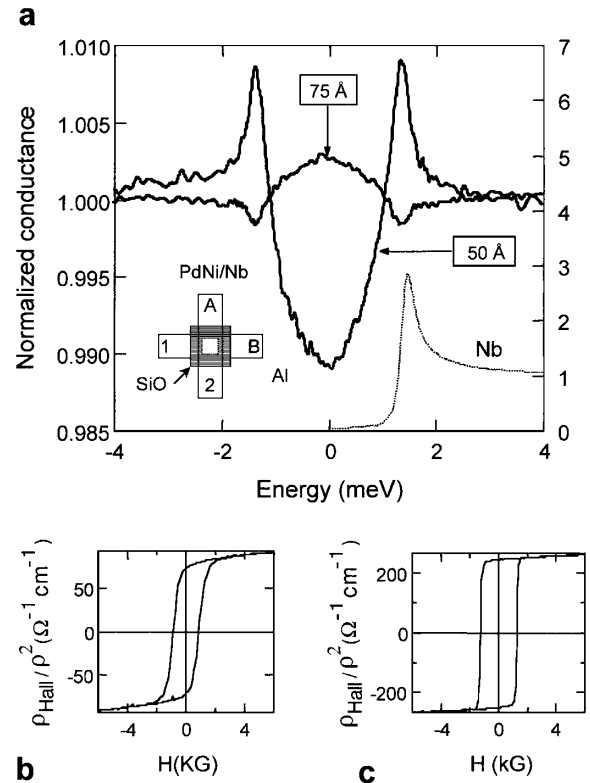


FIG. 2. (a) Differential conductance vs bias for two  $Al/Al_2O_3/PdNi/Nb$  tunnel junctions corresponding to two different thicknesses (50 and 75 Å) of PdNi. The spectra have been taken at  $T = 300$  mK and  $H = 100$  G and normalized by the normal state conductance obtained by applying a magnetic field higher than the Nb critical field. The tunneling spectra show the “0” and “ $\pi$ ” state shapes expected from Fig. 1(a) when the thickness of the ferromagnetic layer is, respectively, smaller or larger than  $\xi_F$ . Note that the induced superconducting density of states is small. The normalized conductance for a tunnel junction without PdNi is also reported on the right-hand side. Inset: junction geometry. The field dependence of the normalized Hall resistivity at  $T = 1.5$  K for the same PdNi films as in the tunnel junctions corresponding to the 0 state (50 Å) and to the  $\pi$  state (75 Å) is shown in (b) and (c), respectively. Long-range magnetic order leads to saturation of the anomalous component of the Hall effect and field-induced hysteresis.

monitored during growth to better than 1 Å by a quartz balance. After depositing 250 Å of SiO on a Si wafer, a 1500-Å-thick aluminum layer was evaporated and quickly oxidized in a 3 min,  $6 \times 10^{-2}$  torr oxygen glow discharge. This produced the Al<sub>2</sub>O<sub>3</sub> tunnel barrier at the Al surface. Tunnel junction areas ( $100 \mu\text{m} \times 100 \mu\text{m}$ ) were defined by evaporating 500 Å of SiO through masks just after oxidation. A PdNi thin layer (thickness 50–100 Å) was then deposited, and backed by a 500 Å layer of Nb ( $T_c = 8.8$  K). PdNi thin films for transport measurements were evaporated simultaneously through a different mask on SiO/Si substrates. Ni concentrations remained about 10%, as checked by Rutherford backscattering spectrometry. Cross-sectional transmission electron microscopy (XTEM) views of the junction before Nb deposition showed some long-distance roughness of the Al layer and PdNi thickness fluctuations  $\approx 20$  Å.

Planar junctions achieve unsurpassed energy resolution and, more importantly in our case, excellent magnitude resolution [12]. In a four-terminal geometry [see inset of Fig. 2(a)], the tunnel conductance is simply obtained by dividing the current driven between 1 and 2 by the signal detected between *A* and *B*. A standard ac-modulation technique is employed [12], the tunneling conductance bias dependence being directly measured as the ac conductance vs the dc signal. High magnitude resolution was obtained via a homebuilt ultralow noise (a few  $nV/\sqrt{\text{Hz}}$ ) dc/ac mixer. The junctions' quality was systematically checked. Reliable spectroscopy requires elastic tunneling and negligible *F/S* interface resistances. Junction resistances were typically between 50 Ω and 1 kΩ, while the *F/S* interface resistance was estimated to be below  $10^{-5}$  Ω by measuring the low energy dissipation ( $V \ll \Delta_s$ ) of Nb/PdNi/Nb junctions. All of the signatures of a high quality spectroscopy were thus obtained; this included a well-developed Al energy gap when the Al was superconducting, the predicted temperature dependence of the tunnel conductance, and the conservation of the number of quasiparticle states. Furthermore, the Nb DOS measured in an Al/Al<sub>2</sub>O<sub>3</sub>/Nb junction with Al in the normal state [see right-hand side of Fig. 2(a)] is that expected from the Bardeen-Cooper-Schrieffer (BCS) theory.

Ferromagnetic order in PdNi alloys results from an indirect exchange between the Ni magnetic moments provided by the large spin susceptibility of Pd [13]. At low Ni concentrations, the total magnetic moment is mainly due to the spin polarized electrons of the host at the Fermi level [14]. Long-range itinerant ferromagnetism provides an almost ideal system where Cooper pairs are suddenly polarized when they enter into the ferromagnet. The main advantage of using a ferromagnetic alloy, instead of pure Ni for instance, is that the exchange energy can be kept suitably small.  $E_{\text{ex}}$  may be estimated from the magnetization  $M \approx \mu_B E_{\text{ex}} \chi$ , where  $\mu_B$  is the Bohr magneton and  $\chi$  is the host susceptibility, if one neglects the contribution of the Ni magnetic moments. In PdNi alloys with

10% of Ni,  $E_{\text{ex}}$  is of the order of 10 meV [15], resulting in  $\xi_F \approx 50$  Å, which corresponds to an order of magnitude increase with respect to pure ferromagnetic elements such as Fe, Ni, or Co. This coherence length is accessible to standard thin film technology. Of course, decreasing the Ni concentration closer to the paramagnetic-ferromagnetic transition would further increase the penetration length of the Cooper pair into the ferromagnet. However, we observed that lowering the Ni concentration results in reduced magnetic homogeneity.

In Fig. 2(a) the superconducting DOS at  $T = 300$  mK is presented for two different thicknesses of PdNi. The Al counterelectrode is driven into the normal state by applying a magnetic field of 100 G perpendicular to the film [16]. The background conductance is obtained by raising the applied field up to 25 kG to quench the Nb superconductivity. For the thinner ferromagnetic layer (50 Å) the phase factor is positive (0 state), and the DOS displays a maximum at the Nb gap edge and a minimum at the Fermi level set to zero in our spectra. As a result of the finite interface resistance between PdNi and Nb, the order parameter is small, corresponding to a few percent difference from the background conductance. To stress that, in our geometry the relevant energy scale for the proximity effect is the Nb gap energy  $\Delta_{\text{Nb}} = 1.40$  meV, as shown in Fig. 2(a). By increasing the thickness of the ferromagnetic layer (75 Å), the phase factor becomes negative ( $\pi$  state) and the DOS is flipped with respect to the normal state [16]. When both electrodes are in the superconducting state (i.e., no applied field) the structures are amplified by the Al BCS singularity and shifted in energy by the aluminum gap, as expected for elastic tunneling.

A check on the magnetic properties of *F* is shown in Figs. 2(b) and 2(c), which present the normalized Hall resistivity,  $\rho_{\text{Hall}}/\rho^2$ , vs the applied field of the 50- and 75-Å-thick PdNi layers, respectively, corresponding to the “0 and  $\pi$  states” measured by tunneling spectroscopy. The Hall effect is sensitive to magnetic scattering through the spin-orbit coupling and provides a suitable probe of weak magnetic moments in the films [17]. In ferromagnetic materials, scattering by defects produces a net asymmetry in the transverse current density that is compensated, at equilibrium, by the anomalous Hall field [18]. The Hall resistivity shows a fast variation at low magnetic field, when the magnetic domains order, and a linear dependence at higher field corresponding to the ordinary Hall effect. As the anomalous Hall effect is proportional to the magnetization and to the square of  $\rho$ , the film resistivity [19], the extrapolation of  $\rho_{\text{Hall}}/\rho^2$  at zero field is proportional to the saturation magnetization. Complementary measurements by the magneto-optical Kerr effect (MOKE) on junctions with the same structure also show ferromagnetic ordering with a typical coercive field,  $H_c$ , of 1500 G close to that measured by the anomalous Hall effect ( $H_c = 1200$  G). Finally, from the direct SQUID measurement of the saturation magnetization we obtain the

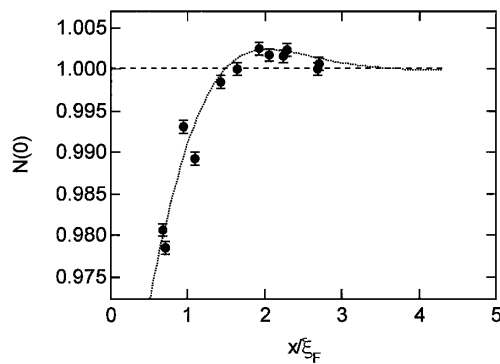


FIG. 3. Tunneling conductance at zero energy vs the PdNi thickness normalized by the coherence length  $\xi_F$ . The data taken at  $T = 300$  mK and  $H = 100$  G are shown as solid symbols. The theoretical curve (dotted line) obtained by solving the Usadel equations in the presence of an exchange field takes into account a finite interface resistance as a fitting parameter. The dashed line denotes the transition from the 0 state to the  $\pi$  state.

exchange energy and hence verify the estimated coherence length in the ferromagnet. We obtain  $M = 0.21\mu_B$  which gives  $E_{\text{ex}} = 15$  meV and  $\xi_F = 45$  Å.

Increasing the thickness of the ferromagnetic layer, i.e., for  $x \gg \xi_F$ , the proximity effect disappears and the normalized tunneling conductance becomes equal to unity. This is shown in Fig. 3 which shows the DOS at zero energy,  $N(0)$ , vs  $x/\xi_F$ .  $\xi_F$  is obtained by measuring the exchange energy from the saturation magnetization as indicated above. For large exchange energies,  $N(0)$  is related to the order parameter  $\Psi$  by the simple formula  $N(0) = \text{Re}\sqrt{1 - \Psi^2}$ . Thus the dependence of  $N(0)$  on the thickness of  $F$  is easily deduced from that of  $\Psi$  shown in Fig. 1(a) [5,20]. In the case of a finite resistance,  $R_B$ , of the  $F/S$  interface the order parameter in  $F$  is reduced by a scale factor  $1/\gamma_B$  as found by solving the Usadel equations for  $\gamma_B \gg 1$  and  $E_{\text{ex}} \gg \Delta_s$ , supplemented by the appropriate  $F/S$  boundary conditions [21].  $\gamma_B$  is a transparency parameter given by  $\gamma_B = R_B/\rho\xi_F$ . The best fit of the data in Fig. 3 is found for  $\gamma_B = 7.5$ , corresponding to an interface resistance  $R_B \approx 10^{-6}$  Ω, consistent with the upper limit estimated directly from the  $I/V$  curves. In the fit the spatial coordinate,  $x$ , is shifted by 15 Å, suggesting that the actual ferromagnetic thickness is reduced with respect to its nominal value. This may be a consequence of the fluctuations in the thickness of  $F$  as observed by XTEM or/and to some interdiffusion at the  $F/S$  interface as shown by x-ray reflectivity measurements [22].

Our results show that the superconducting order parameter induced into a ferromagnet by proximity effects oscillates with a period given by the exchange energy. They suggest that  $S/F$  nanostructures offer a unique way to investigate the interplay between superconductivity and magnetic order since they do not require comparable en-

ergy scales. Furthermore, they indicate that the proximity effect may indeed be used to fabricate Josephson junctions with a  $\pi$ -phase shift, as recently proposed [23].

We are indebted to P. Veillet, P. Monod, and J. Ferré for the SQUID and MOKE magnetic characterization, to W. Guichard and P. Gandit for measuring the Nb/PdNi/Nb interface resistance, and to S. Collin and O. Kaitasov for the TEM analysis. We also thank D. Esteve, H. Pothier, W. Belzig, Yu. Nazarov, A. Buzdin, J-P. Torre, O. Bourgeois, and H. Bernas for useful discussions.

- [1] D. J. Van Harlingen, *Rev. Mod. Phys.* **67**, 515 (1995).
- [2] P. Fulde and A. Ferrel, *Phys. Rev.* **135**, A550 (1964).
- [3] A. Larkin and Y. Ovchinnikov, *Sov. Phys. JETP* **20**, 762 (1965).
- [4] M. A. Clogston, *Phys. Rev. Lett.* **9**, 266 (1962).
- [5] E. A. Demler, G. B. Arnold, and M. R. Beasley, *Phys. Rev. B* **55**, 15 174 (1997).
- [6] We calculated the spatial dependence of the induced order parameter and the superconducting density of states solving the Usadel equations in the presence of an exchange field [5]. As described in the text the oscillations occur in either the ballistic or the diffusion limit (W. Belzig *et al.*, cond-mat/0010089). Note that a finite interface resistance reduces the proximity effect, lowering the order parameter amplitude and the superconducting density of states.
- [7] A. F. Andreev, *Sov. Phys. JETP* **19**, 1228 (1964).
- [8] M. J. M. de Jong and C. W. J. Beenakker, *Phys. Rev. Lett.* **74**, 1657 (1995).
- [9] R. J. Soulen, Jr. *et al.*, *Science* **282**, 85 (1998).
- [10] J. M. Rowell and W. L. McMillan, *Phys. Rev. Lett.* **16**, 453 (1966).
- [11] S. Guéron *et al.*, *Phys. Rev. Lett.* **77**, 3025 (1996).
- [12] E. L. Wolf, *Principles of Electron Tunneling Spectroscopy* (Oxford University Press, New York, 1985).
- [13] A. P. Murani, A. Tari, and B. R. Coles, *J. Phys. F* **4**, 1769 (1974).
- [14] T. Takahashi and M. Shimizu, *J. Phys. Soc. Jpn.* **20**, 26 (1965).
- [15] J. Beille, Thèse de troisième cycle, Université J. Fourier, Grenoble, 1975.
- [16] Spectra taken at  $T = 1.5$  K in zero magnetic field show the same behavior. Furthermore, no effects of domain ordering ( $H < 1$  kG) has been observed.
- [17] G. Bergmann, *Phys. Rev. Lett.* **41**, 264 (1978).
- [18] C. M. Hurd, *The Hall Effect in Metals and alloys* (Plenum, New York, 1972).
- [19] L. Berger and G. Bergmann, *The Hall Effect and Its Applications*, edited by C. L. Chien and C. R. Westgate (Plenum, New York, 1980).
- [20] A. Buzdin, *Phys. Rev. B* **62**, 11 377 (2000).
- [21] J. Aarts *et al.*, *Phys. Rev. B* **56**, 2779 (1997).
- [22] C. Coccorese *et al.*, *Phys. Rev. B* **58**, 7922 (1998).
- [23] A. I. Buzdin, B. Bujcic, and M. Yu. Kupriyanov, *Zh. Eksp. Teor. Fiz.* **101**, 231 (1992).